

1 **Title: The scorpionfly (*Panorpa cognata*) genome highlights conserved and derived**
2 **features of the peculiar dipteran X chromosome.**

3

4 **Running title:** The scorpionfly genome and dipteran X

5

6 **Authors:** Clementine Lasne^{1*} & Marwan Elkrewi^{1*}, Melissa A. Toups², Lorena Layana¹,
7 Ariana Macon¹, Beatriz Vicoso¹

8

9 ¹ Institute of Science and Technology Austria (ISTA)

10 ² Bournemouth University, UK

11 * co first-authors

12

13 **Corresponding authors:**

14 Clementine Lasne: clementine.lasne@gmail.com

15 Beatriz Vicoso: bvicoso@ist.ac.at

16

17 **Key words:** insects, sex-chromosome evolution, Muller element F, scorpionflies

18

19 **Abstract**

20

21 Many insects carry an ancient X chromosome - the *Drosophila* Muller element F - that likely
22 predates their origin. Interestingly, the X has undergone turnover in multiple fly species
23 (Diptera) after being conserved for more than 450 MY. The long evolutionary distance between
24 Diptera and other sequenced insect clades makes it difficult to infer what could have
25 contributed to this sudden increase in rate of turnover. Here, we produce the first genome and
26 transcriptome of a long overlooked sister-order to Diptera: Mecoptera. We compare the
27 scorpionfly *Panorpa cognata* X-chromosome gene content, expression, and structure, to that

28 of several dipteran species as well as more distantly-related insect orders (Orthoptera and
29 Blattodea). We find high conservation of gene content between the mecopteran X and the
30 dipteran Muller F element, as well as several shared biological features, such as the presence
31 of dosage compensation and a low amount of genetic diversity, consistent with a low
32 recombination rate. However, the two homologous X chromosomes differ strikingly in their
33 size and number of genes they carry. Our results therefore support a common ancestry of the
34 mecopteran and ancestral dipteran X chromosomes, and suggest that Muller element F
35 shrank in size and gene content after the split of Diptera and Mecoptera, which may have
36 contributed to its turnover in dipteran insects.

37

38 **Introduction**

39

40 Sex chromosomes originally arise from autosomes (Muller 1914; Ohno 1967), but over time
41 can evolve highly specialized sequence and regulatory features. Loss of recombination
42 between nascent X and Y chromosomes often leads to genetic degeneration of the Y, which
43 becomes gene-poor and enriched for transposable elements and other repeats (Charlesworth
44 et al. 1994). This degeneration can cause gene expression imbalances between X-linked and
45 autosomal genes in the heterogametic sex, which in turn select for the evolution of dosage
46 compensation mechanisms that re-establish optimal X:autosomes expression balance, such
47 as doubling the expression of the male X in *D. melanogaster* (Gupta et al. 2006). Finally, insect
48 X chromosomes are often enriched for genes that are primarily expressed in females (female-
49 biased genes), and depleted of male-biased genes (Parisi et al. 2003; Mikhaylova and
50 Nurminsky 2011; Pal and Vicoso 2015; Whittle et al. 2020; Parker et al. 2022). Due to these
51 unusual features, highly differentiated sex chromosomes are thought to be difficult to revert to
52 autosomes and to be maintained over long periods of time, or even become non-reversible
53 “evolutionary traps” (Pokorná and Kratochvíl 2009). The growing pool of genomic and
54 transcriptomic data for both model and non-model organisms has provided support for the

55 long-term existence of stable sex chromosomes with highly conserved gene content across
56 entire clades - such as the XY chromosomes of eutherian mammals and the avian ZW
57 chromosomes (Marshall Graves 2016; Vicoso 2019), but also uncovered clades with high
58 rates of sex-chromosome turnovers between closely related species, e.g. frogs (Jeffries et al.
59 2018), cichlids (El Taher et al. 2021) and crustaceans (Becking et al. 2017). It remains unclear
60 why some taxa acquire highly conserved sex chromosomes and others have very high rates
61 of turnover.

62

63 Insects are an excellent taxon to study both conservation and turnover of sex chromosomes.
64 They show both male- and female-heterogametic systems, as well as tremendous variation in
65 the extent of sex-chromosome (and gene content) conservation between different orders
66 (Blackmon et al. 2017). Recurrent sex-chromosome turnover has occurred in flies (Diptera),
67 where the ancestral sex chromosome (the dipteran “Muller element F”) has been replaced as
68 the X by another chromosome multiple times independently (Vicoso and Bachtrog 2013;
69 Vicoso and Bachtrog 2015). On the other hand, conservation of the X chromosome has been
70 observed in Hemipterans (Pal and Vicoso 2015) and Coleoptera (Bracewell et al. 2023). The
71 most striking evidence of conservation so far is the apparent homology between the X
72 chromosomes of the cockroach (Blattodea) (Meisel et al. 2019), the damselfly (Chauhan et al.
73 2021), the grasshopper (Orthoptera) (Li et al. 2022) and the ancestral dipteran X chromosome
74 - element F, suggesting that the same X chromosome has been maintained for over 400
75 millions years of evolution. Why such an ancient and well conserved sex chromosome would
76 undergo repeated turnover in Diptera is unclear, but may have to do with its reduced size and
77 gene content in this clade, which should mitigate the fitness consequences of reverting it to
78 an autosome (Vicoso 2019; Toups and Vicoso 2023). However, due to the very large
79 evolutionary distances between these insects, it is difficult to conclusively disentangle whether
80 there is long-standing conservation of Muller element F as the X chromosome across insect
81 orders, or if this represents the convergent recruitment of the same set of genes for sex

82 determination. Element F is also known to have an unusual biology in *Drosophila*
83 *melanogaster*, where it has been studied extensively: it is almost entirely heterochromatic and
84 does not undergo crossing over (and consequently has an extremely low recombination rate).
85 Whether these features are related to its small size and/or turnover as the X chromosome is
86 unclear, since no close outgroup of Diptera carrying element F as the X has been
87 characterized.

88

89 Relatively few molecular and genomic resources are available for Mecoptera - the sister-order
90 to Diptera that comprises scorpionflies and hangingflies (Misof et al. 2014). Cytogenetic
91 studies show that almost all Mecoptera species studied so far are XX/XO (Miao et al. 2019),
92 but the mecopteran X chromosome has not yet been characterised at the molecular level.
93 Intriguingly, it has been described as “dot-shaped” in meiotic spreads of several *Panorpa*
94 scorpionfly species (Xu et al. 2013), a term that is reminiscent of the shape of Muller element
95 F in *Drosophila* (where it is also known as the “dot chromosome” (Ashburner et al. 2005)),
96 making scorpionflies a promising model for understanding the evolution of the peculiar
97 element F. We produced a high-quality genome assembly from PacBio reads for the
98 scorpionfly species *Panorpa cognata* (order: Mecoptera). We identified X-derived scaffolds,
99 and inferred the level of conservation of gene content of the X chromosome between this clade
100 and various dipteran and non-dipteran insects. We combined our genome assembly with
101 extensive transcriptomic data to explore patterns of dosage compensation in different tissues
102 and tissue-specificity of X and autosomal genes. Finally, we investigated whether the *P.*
103 *cognata* X showed features of a heterochromatic chromosome, similar to Muller element F.

104

105 **Methods**

106

107 Sample collection and sequencing

108 *P. cognata* specimens were collected in August 2021 in Maria Gugging (Lower Austria) and
109 immediately frozen at -80°C until further processing. Species identification was confirmed by
110 sequencing the mitochondrial cytochrome c oxidase I (COI) gene and comparing it to available
111 sequences for this species (Misof et al. 2000). High molecular weight DNA was extracted from
112 a single male with the Qiagen Genomic-Tip 100/G Kit, and used for PacBio long read DNA
113 sequencing. A single frozen female was used for Hi-C library prep and illumina sequencing.
114 For illumina whole genome sequencing, DNA was extracted from 1 male and 1 female
115 separately using the Qiagen DNeasy Blood and Tissue kit and fragmented using the Bioruptor
116 Plus Ultrasonicator. Total RNA was extracted from the heads, gonads and carcasses of the 3
117 males and 3 females (samples were not pooled) using the Bioline Isolate II RNA extraction kit,
118 resulting in 3 biological replicate samples per tissue and sex and a total of 18 libraries. All DNA
119 and RNA sequencing libraries were prepared and sequenced at the Vienna Biocenter
120 Sequencing Facility. All RNA and DNA samples used for the downstream transcriptome
121 assembly and gene expression analysis are listed in **Table S1**, and the corresponding
122 sequencing reads are available at the NCBI Short Reads Archive under Bioproject number
123 PRJNA989034.

124

125 **Genome assembly**

126 PacBio consensus reads were generated from the raw bam file using the PacBio CCS tool
127 (version 6.4.0, on conda 4.14.0). The CCS reads were assembled using Hifiasm (version 0.15-
128 r327; (Cheng et al. 2021)), and the primary assembly was purged using purge_dups (version
129 1.2.5; (Guan et al. 2020)) to remove any duplicate sequences. The Hi-C reads were then
130 aligned to contigs longer than the N80 of the assembly (as smaller contigs still appeared to be
131 largely redundant), and processed using the HiC-Pro pipeline (version 3.1.0; (Servant et al.
132 2015)). The valid alignments were extracted from the resulting bam file, further filtered for edit
133 distance (NM:i:0) using Matlock (phase genomics), and then used for scaffolding the purged
134 primary assembly with YaHS (YaHS-1.2a.1.patch; (Zhou et al. 2023)). BUSCO was used to

135 assess the completeness of the genome with the arthropoda_odb10 dataset (version 5.4.4;
136 (Manni et al. 2021)). As most of the genome is contained in super-scaffolds, we performed
137 downstream analyses using the longest 25 scaffolds (**Table S2**). The choice of scaffold
138 number was mainly based on the large drop in length after the 25th scaffold and supported by
139 the minor decrease in BUSCO score (**Figure S1**).

140

141 **Identification of X-linked scaffolds**

142 The *P. cognata* female and male Illumina DNA reads were mapped to the assembled genome
143 using Bowtie2 (version 2/2.4.5; (Langmead and Salzberg 2012)) with end-to-end sensitive
144 mode. SOAP.coverage (version 2.7.7; <https://github.com/gigascience/bgi-soap2/tree/master/tools/soap.coverage>) was used to calculate the genomic coverage for each scaffold in
145 windows of 10000 bp from the resulting SAM alignment. The \log_2 of the ratio of male to female
146 coverage was calculated for all the windows and the $[\text{median}(\log_2(\text{Male/Female coverage})) -$
147 $0.5]$ was used as a cut-off to assign scaffolds as either X-linked or autosomal. If the
148 $\text{median}(\log_2(\text{Male/Female coverage}))$ for the scaffold windows was below the cut-off, the
149 scaffold was assigned as X-linked, otherwise it was assigned as an autosome.

151

152 **Transcriptome assembly and transcripts genomic location**

153 The *P. cognata* transcriptome was assembled from all 18 RNA-seq libraries. Quality control of
154 the paired-end reads was conducted using FastQC (version 0.11.9; (Andrews 2010)) and
155 quality filtering with TRIMOMATIC (version 0.36; (Bolger et al. 2014)). We used Trinity
156 (trinityrnaseq-v2.11.0; (Grabherr et al. 2011)) and Evigene (EvidentialGene tr2aacds.pl
157 version 2022.01.20; (Gilbert 2016)) to assemble and curate the transcriptome, and further
158 filtered for transcript sequence-length greater than 500bp using fafilter (UCSC source code
159 collection, <http://genome.ucsc.edu/>). The transcriptome assembly quality was checked with
160 BUSCO using arthropoda_odb10 as a reference dataset (version 5.4.4; (Manni et al. 2021)).

161 The final transcriptome assembly consists of 36618 transcripts and is available at the ISTA
162 data repository [*a permanent URL will be added upon acceptance*].

163
164 To determine the genomic location of each transcript, we mapped our transcriptome to our
165 genome assembly with Standalone BLAT (version 36x2; (Kent 2002)). We used custom Perl
166 scripts to keep only the best hit for each gene in the genome and, when multiple transcripts
167 overlapped on the genome, to keep only the transcript with the highest mapping score (unless
168 they overlapped by less than 20 bps, in which case both were kept).

169
170 **Homology of the *Panorpa cognata* and *Cochliomyia hominivorax* X chromosomes**
171 The *P. cognata* protein sequences were obtained from the transcriptome using a Perl script
172 (GetLongestAA_v1_July2020.pl), which outputs the longest amino acid sequence for each *P.*
173 *cognata* transcript. The published annotation file (GFF) and genome of the New World
174 screwworm *Cochliomyia hominivorax* (order: Diptera; suborder: Brachycera) were obtained
175 from Dryad (Scott 2022). The protein sequences of *C. hominivorax* were extracted from the
176 GFF and genome files using gffread (version 0.12.7; (Pertea and Pertea 2020)) and were
177 filtered with a Perl script (GetLongestCDS_v2.pl) to get the longest isoform per protein. The
178 correspondence between Muller elements and *C. hominivorax* chromosomes was obtained
179 from Tandonnet et al. (2023). Since an outgroup was required to obtain orthologous genes
180 between the two species, the protein sequences of the yellow fever mosquito *Aedes aegypti*
181 (order: Diptera; suborder: Nematocera) were retrieved from Ensembl Metazoa (and were also
182 filtered with the Perl script mentioned above).

183
184 We then used Orthofinder (Emms and Kelly 2019) to obtain 1-to-1 orthologous genes between
185 *C. hominivorax* and *P. cognata*, and calculated the proportion of these 1-to-1 orthologs that
186 were X-linked in *P. cognata* (hereafter “X-linkage threshold”). We then estimated the
187 proportion of *P. cognata* genes that are X-linked separately for 1-to-1 orthologs that are on

188 each Muller element of *C. hominivorax*. We performed a chi-squared test comparing the
189 proportion obtained for each Muller element to the proportion obtained from all the others (e.g.
190 element A versus elements B,C,D,E,F), using the Python function
191 `scipy.stats.chi2_contingency` from SciPy library (Virtanen et al. 2020). Muller elements that
192 had a significant p-value ($P < 0.05$) and were above “the X-linkage threshold” were considered
193 as overrepresented. We also performed this analysis using *Drosophila melanogaster*
194 (**Methods S1**).

195

196 **Conservation of X-linked gene content between *P. cognata* and other insects**

197 We assessed whether the X-linked genes of *P. cognata* were also present on the X
198 chromosome of two other insect species: the migratory locust *Locusta migratoria* (Order:
199 Orthoptera) and the spotted crane fly *Nephrotoma appendiculata* (suborder: Nematocera, a
200 basal dipteran known to have element F as the X). The tree representing the phylogenetic
201 relationship between these species was generated using the online tool iTol
202 (<https://itol.embl.de/about.cgi>, version 6.7.3) based on the topology of Misof et al. (2014).
203 Since a genome annotation was not available for these species we used a pipeline that
204 bypassed the need for protein sequences to infer homology between X chromosomes. We
205 downloaded chromosome-level genome assemblies from the National Center for
206 Biotechnology Information (NCBI) for *L. migratoria*
207 (https://www.ncbi.nlm.nih.gov/assembly/GCA_026315105.1/) and *N. appendiculata*
208 (https://www.ncbi.nlm.nih.gov/assembly/GCA_947310385.1/). We then used Standalone
209 BLAT (version 36x2; (Kent 2002)) to map our *P. cognata* transcriptome to the genome of these
210 two species using a translated query and database, and filtered for hits with a match score
211 above 50. A Perl script (1-besthitblat.pl) was then used to get only the best hit for each
212 transcript in the genome, and another Perl script (2-redremov_blat_V2.pl) to keep only the
213 transcript with the highest mapping score when two transcripts overlapped by more than

214 20bps. We used this set of *P. cognata* transcripts, with their genomic location in *L. migratoria*
215 and *N. appendiculata*, as a proxy for the location of orthologous genes.

216

217 **Synteny of *P. cognata*, *C. hominivorax* and *N. appendiculata***

218 Synteny was examined between *P. cognata* and two dipteran species, *C. hominivorax* and *N.*
219 *appendiculata*, using GENESPACE (version 0.94; (Lovell et al. 2022)), which requires a GFF
220 annotation and a set of peptide sequences for each species. For *C. hominivorax*, we used the
221 GFF provided by the *C. hominivorax* genome project and the peptide sequences produced as
222 described above as input. For the other species, new amino acid sequences that met the
223 GENESPACE input requirements were obtained. We obtained a genome annotation for *P.*
224 *cognata* by mapping the RNA-seq libraries to the genome using HISAT2 (version 2.2; (Kim et
225 al. 2019)). GTF files were generated for each library and then merged together using
226 StringTie2 (version 2.2.1; (Kovaka et al. 2019)). The resulting GTF file was then converted to
227 the GFF3 format using the gffread command from the cufflinks package (cufflinks version
228 2.2.1; (Trapnell et al. 2010)). We input the StringTie GTF file produced above into
229 Transdecoder (version 5.5 ; Haas, BJ. <https://github.com/TransDecoder/TransDecoder>) to
230 select the longest ORFs. We then searched for homology between our ORFs and the uniprot
231 database (The UniProt Consortium et al. 2023) using ncbi blast (version 2.2.31; (Camacho et
232 al. 2009)). Blast results were integrated into Transdecoder (version 5.5.0; Haas, BJ.
233 <https://github.com/TransDecoder/TransDecoder>) protein prediction. We then selected the
234 longest isoform using a custom Perl script.

235

236 To generate peptide sequences for *N. appendiculata* and *L. migratoria*, we first downloaded
237 RNAseq for each species (ERR10378025 ([https://www.ncbi.nlm.nih.gov/sra/?term=](https://www.ncbi.nlm.nih.gov/sra/?term=ERR10378025)
238 ERR10378025)) and SRR22110765 (Li et al. 2022), respectively) from the Sequence Read
239 Archive hosted by NCBI. Quality was assessed using FastQC
240 (<https://www.bioinformatics.babraham.ac.uk/projects/fastqc/>). Reads were quality trimmed

241 and adapters were removed with Trimmomatic (version 0.39; (Bolger et al. 2014)). We then
242 proceeded with the pipeline described in the previous paragraph for *P. cognata* to produce a
243 GFF file and peptide sequences for the longest isoform of each gene.

244

245 **Gene expression and dosage compensation**

246

247 *Quantification and normalisation*

248 The newly assembled *P. congata* transcriptome was indexed with Kallisto (version 0.46.2;
249 (Bray et al. 2016)). The trimmed RNA-seq reads of all 18 samples were mapped to the
250 transcriptome and gene expression was quantified using the same program. Only transcripts
251 mapping to the largest 25 scaffolds in the genome were retained for further analyses. Further
252 gene expression and statistical analyses were performed in R (R Core Team 2020). We
253 performed quantile normalisation of gene expression (in Transcripts Per Million, TPM) across
254 all 18 samples using the R package NormalizerDE (version 1.16.0; (Willforss et al. 2019)). We
255 then visualised the overall similarity in expression profiles of our samples using the Spearman
256 correlation option embedded in the function heatmap.2 of the R package gplots (version 3.1.3;
257 <https://github.com/talgalili/gplots>).

258

259 *Dosage compensation*

260 For each tissue, gene expression was first normalised across male and female samples, then
261 averaged within each sex. A second quantile normalisation was applied to these sex averages,
262 and only genes with expression levels > 0.5 TPM in both sexes were kept for comparing
263 expression patterns between the X and autosomes. Significant differences in gene expression
264 values between sexes and chromosomes were tested for using Wilcoxon rank sum tests.

265

266 *Tissue-specific expression*

267 Tissue-specific expression of autosomal and X-linked genes was assessed by averaging gene
268 expression across both sexes for heads and for carcasses, but separately for gonads to obtain
269 testis-specific and ovary-specific gene expression. A gene was considered as tissue-specific
270 if its expression level was greater than 1 TPM in a tissue and smaller than 0.5 TPM in all other
271 tissues. Significant differences in the proportions of tissue-specific genes between the X and
272 the autosomes were assessed using the chi-squared test option in the
273 pairwiseNominalIndependence function of the R package rcompanion (version 2.4.21;
274 (Mangiafico 2023)).

275

276 *Sex-biased gene expression*

277 Genes that are differentially expressed between the two sexes in gonads, heads, and
278 carcasses were called using the R package sleuth (Pimentel et al. 2017). Genes with q-values
279 < 0.05, a TPM value > 0.5 in both sexes and a 2-fold differential expression between the sexes
280 were considered sex-biased. Significant differences in the proportions of sex-biased genes
281 between the X and the autosomes were assessed using the chi-squared test option in the
282 pairwiseNominalIndependence function of the R package rcompanion. Statistical analyses
283 could not be conducted in head and carcass, as too few genes were sex-biased in these
284 tissues.

285

286 **GC content and nucleotide diversity**

287 GC content was estimated for 10000 bp windows along the genome scaffolds using the
288 GCcalc.py script (<https://github.com/WenchaoLin/GCcalc>). To assess the nucleotide diversity
289 of the transcriptome, the RNAseq reads were first aligned to the transcriptome using bwa-
290 mem (Li 2013), and then SNPs were called using bcftools (Danecek et al. 2021) and filtered
291 using vcftools (Danecek et al. 2011). The filtered vcf file was then used as input to PIXY
292 (Korunes and Samuk 2021), which calculates the population genetic summary statistic pi (π),

293 with a sliding window size of 28kb (corresponding to the largest transcript in our data, such
294 that we obtained one value of pi per transcript).

295

296 **Repeat Content**

297 A consensus repeat library was generated and annotated using RepeatModeler (version 2.0.4;
298 (Flynn et al. 2020)). The repeat library was used with RepeatMasker (version 4.1.5; (Smit et
299 al. 2013)) to get a detailed annotation of the repeat content across the genome. The
300 proportion of repeats were obtained for windows of 10000 bp from the output of RepeatMasker
301 using a custom Python script.

302

303 **Results**

304

305 **Genome assembly and identification of the X**

306 We produced the first mecopteran genome assembly for the species *P. cognata*, using PacBio
307 reads from a single male and illumina Hi-C reads from a single female. The final genome
308 assembly contains 187 scaffolds, and the estimated genome size is 0.46 GB. The BUSCO
309 analysis revealed a 99% genome assembly completeness (**Figure S1**, left panel). Although
310 the assembly is not chromosome-level (cytogenetic studies of *P. cognata* reported n=22
311 chromosomes (Miao et al. 2019)), potentially due to the low complexity/quality of the Hi-C
312 data, most of the genome is contained in super-scaffolds. In particular, 73% of the genome is
313 in the longest 25 scaffolds, which we focus on for the rest of the manuscript (the corresponding
314 BUSCO score is 93%). Based on their reduced ratio of male to female short read genomic
315 coverage, two super-scaffolds (scaffold_1 and scaffold_22) and a few smaller scaffolds were
316 identified as X-linked (**Figure 1**). The absence of scaffolds with male-specific coverage in the
317 genome assembly supports the lack of a Y chromosome in *P. cognata* (**Figure S2**).

318

319 **Conservation of the X chromosome**

320 To identify X-linked genes, we assembled a transcriptome (see methods and next section),
321 which we mapped to the *P. cognata* genome. Of the 13214 non-redundant mapped transcripts,
322 a proxy for individual genes, 1520 (11.5%) mapped to X-linked scaffolds, showing that the X
323 is one of the largest and most gene-rich chromosomes in this species. We then investigated
324 whether this X chromosome was homologous to the X of several other insects (**Figure 2(a)**).

325

326 We first tested for homology between the *P. cognata* and dipteran X chromosomes by
327 detecting 1-to-1 orthologs with the screwworm *C. hominivorax*, a dipteran species that has
328 maintained the ancestral element F as the X. **Figure 2(b)** shows that *C. hominivorax* genes
329 located on the X-linked element F, and to a lesser extent on the autosomal element E, are
330 significantly overrepresented among *P. cognata* X-linked genes. The overrepresentation of
331 those elements also holds when taking into account all the scaffolds in our *P. cognata* genome
332 (**Figure S3(a)**) and when *D. melanogaster* is used as the dipteran outgroup (**Figure S4**). The
333 synteny plot between the *C. hominivorax* genome and the 25 largest scaffolds from our *P.*
334 *cognata* genome (**Figure 2(e)**) supports the homology of the *P. cognata* X-linked scaffolds 1
335 and 22 to Muller elements E and F in *C. hominivorax*, despite the poor conservation of synteny
336 overall.

337

338 The previous results show that, while the *P. cognata* and dipteran X chromosomes are
339 homologous, many *P. cognata* X-linked genes are derived from other Muller elements. We
340 first set out to test if this additional gene content of the X reflects the ancestral state of insects,
341 or instead corresponds to an increase in X-linked gene content in the *P. cognata* lineage. To
342 do so, we divided the *P. cognata* X-linked genes into two based on the location of their
343 homologues in the *C. hominivorax* genome: a set homologous to dipteran element F genes
344 ("X in F"), and a set homologous to genes on other chromosomes ("X not F"). We then
345 estimated the proportion of the two sets that are also X-linked in the distant outgroup *L.*
346 *migratoria* (and *B. germanica* in **Figure S5**). **Figure 2(d)** shows that the percentage of "X not

347 F" genes that are also X-linked in *L. migratoria* (~45%) is greater than the corresponding
348 percentage for *P. cognata* autosomal genes (<10%, $P < 0.001$, chi-squared test), suggesting
349 that the difference in gene content reflects at least partly a loss of X-linked genes in dipterans
350 (in agreement with (Toups and Vicoso 2023)). We performed a similar analysis with *N.*
351 *appendiculata*, a dipteran species that is a putative outgroup to flies and mosquitoes, to
352 investigate if the shrinking of the X occurred early in dipteran evolution, or later in the
353 Brachycera ("higher dipterans"). While there is still an excess of *P. cognata* "X not F" genes
354 on the *N. appendiculata* X ($P < 0.001$, chi-squared test), the percentage (~10%) is much lower
355 than in the previous analysis with the locust. This suggests that much of the loss of genes in
356 the ancestral X chromosome of Diptera occurred at some point before the split of
357 Tipulidae. We obtained similar results when we considered all the scaffolds in our *P. cognata*
358 genome (**Figure S3(b-c)**).

359

360 **Gene expression of the X, dosage compensation, and gene content**

361 The *P. cognata* transcriptome was assembled by pooling male and female head, gonad, and
362 carcass samples (See Methods). The final transcriptome contains 36618 transcripts and has
363 an N50 of 1329 bp. The completeness of our transcriptome assembly was estimated to 92.7%
364 according to our BUSCO analysis (**Figure S1**, right panel). All subsequent analyses of the
365 gene expression data were conducted using the 12357 transcripts of known location on the
366 first 25 genome scaffolds: 11083 on the autosomes and 1274 on the X. A Spearman
367 correlation analysis confirmed that the RNA-seq samples cluster together according to tissues,
368 and according to sex within the gonad and carcass clusters (**Figure S6**).

369

370 We compared male and female gene expression on the autosomes and on the X in heads, a
371 somatic organ, and gonads, to assess patterns of dosage compensation and sex-biased
372 expression in scorpionflies (**Figure 3**). We found no difference in expression between
373 autosomal and X-linked genes, nor between the sexes, in heads (**Figure 3(a)**). The male-

374 over-female expression ratio was also similar between autosomal and X-linked genes in this
375 tissue (**Figure 3(c)**), confirming that the X chromosome is fully compensated. In gonads, the
376 expression of X-linked genes was significantly lower in males relative to females ($P < 0.001$,
377 Wilcoxon rank sum test ; **Figure 3(b)**) and relative to male autosomal genes ($P < 0.001$,
378 Wilcoxon rank sum test). The male-over-female expression ratio of the X chromosome was
379 also significantly lower than that of autosomes ($P < 0.001$, Wilcoxon rank sum test; **Figure**
380 **3(d)**), suggesting that either dosage compensation is incomplete in this tissue, or that a
381 differential accumulation of genes with sex-biased expression has occurred on the X
382 chromosome (see below). Similarly to heads, we found evidence of dosage compensation in
383 carcasses (**Figure S7**).

384

385 The *Drosophila* gene *Painting-of-fourth* (*POF*) has been shown to mediate dosage
386 compensation in the sheep blowfly, *Lucilia cuprina*, a dipteran species with the ancestral
387 element F as the X. Given the homology between the *P. cognata* and dipteran X
388 chromosomes, we investigated whether *POF* showed patterns of expression consistent with
389 a role in dosage compensation in scorpionflies, i.e. whether it was expressed primarily in male
390 somatic tissues, but less so in testis and in female tissues. Contrary to this, *POF* seemed to
391 be expressed at similar levels heads of both sexes and in ovaries, but showed reduced
392 expression in testes and to some extent in carcasses (**Figure S8**).

393

394 Finally, X chromosomes often differ from autosomes in the proportion of sex-biased, tissue-
395 and sex-specific genes that they carry. We found an excess of female-biased genes on the X
396 relative to the autosomes in gonads: 31.6% and 24.1%, respectively ($adj\ P < 0.01$, chi-squared
397 test; **Figure 3(e)**). We also observed a paucity of male-biased genes on the X (6.1%) relative
398 to the autosomes (11.9%) ($adj\ P < 0.001$, chi-squared test). Fewer than 50 genes were found
399 to be sex-biased in carcasses, and only one gene in heads, such that no comparisons between
400 the X and the autosomes were possible. We also investigated the extent to which X-linked

401 and autosomal genes show tissue-specific expression. We found a significantly greater
402 proportion of genes with ovary-specific expression on the X chromosome relative to the
403 autosomes: 5.34% and 2.09% of genes, respectively (*adj. P* < 0.001, chi-squared test; **Figure**
404 **3(f)**). However, there was no difference in gene-specificity between the X and autosomes in
405 heads and testes, and we note a high percentage of testis-specific genes on the X (7.54%).
406 Finally, the percentage of genes showing carcass-specific expression was significantly lower
407 on the X relative to the autosomes: 0.7% and 2.44%, respectively (*adj. P* < 0.001, chi-squared
408 test).

409

410 **X vs. autosomal genetic diversity, CG and repeat content**

411 Muller element F, which corresponds to the ancestral dipteran X, is non-recombining and
412 largely heterochromatic in *Drosophila*. We investigated whether these features might have
413 already been present in the X of the ancestor of dipterans and mecopterans. We compared
414 autosomal and X-linked pairwise nucleotide diversity (π) and found that autosomal scaffolds
415 have higher levels of genetic diversity than X-linked scaffolds in both sexes (P < 0.001,
416 Wilcoxon rank sum test; **Figure 4(a)** for females). The X/Autosome diversity is 0.23 in females,
417 and 0.12 in males, well below the expectation of X/Autosome = 0.75 (the null hypothesis when
418 only the number of copies of X chromosomes and autosomes in a population are considered),
419 consistent with a low recombination rate of the X. GC content, which is also correlated with
420 recombination rate (Charlesworth et al. 2020), is also lower on the X relative to the autosomes
421 (P < 0.001, Wilcoxon rank sum test; **Figure 4(b)**). Finally, the density of repeats is higher on
422 the X relative to the autosomes (P < 0.001, Wilcoxon rank sum test; **Figure 4(c)**), again
423 consistent with low recombination and/or a higher density of constitutive heterochromatin.
424 **Figure S9** presents these results per scaffold. Interestingly, the nature of repeats appears to
425 differ between the X and the autosomes. While the former seems to have a high proportion of
426 DNA transposons, the autosomes seem to have a higher proportion of retrotransposons
427 (**Table S3**).

428

429 **Discussion**

430

431 **Conservation of the Diptera Muller element F**

432 Our results show that the *P. cognata* X chromosome is homologous to the X of Orthoptera
433 and Blattodea, as well as to the ancient X chromosome of Diptera - Muller element F,
434 consistent with the finding of high conservation of the X chromosome across numerous insect
435 taxa (Meisel et al. 2019; Chauhan et al. 2021; Li et al. 2022; Toups and Vicoso 2023). Despite
436 the homology between the scorpionfly and dipteran X chromosomes, the two chromosomes
437 differ at several key features. First, the dipteran Muller element F is known for its small size;
438 the *P. cognata* X is a much larger chromosome and contains over 1000 genes. This nicely
439 illustrates how "homologous chromosomes" can acquire vastly different gene contents over
440 time due to inter- and intrachromosomal rearrangements, and supports the idea that shrinking
441 of the dipteran X may have driven its high rate of turnover (Toups and Vicoso 2023). Second,
442 our *P. cognata* genome assembly is consistent with a XX/XO male-heterogametic system, as
443 no scaffolds showed male-specific genomic coverage. The absence of a Y chromosome
444 necessarily implies that sex determination is dosage-dependent, either through the
445 X:autosome ratio - as in *Drosophila* (Gilbert 2000), or through the number of X chromosomes
446 present in an individual (Blackmon et al. 2017). Because sex-determination is controlled by a
447 Y-linked male-determining factor in some dipterans using the ancestral element F as their X
448 (Sharma et al. 2017; Meccariello et al. 2019; Fan et al. 2023), genes controlling the primary
449 sex determination signal are likely different between Diptera and Mecoptera. This illustrates
450 how the sex determination signal can change even when homology of the sex chromosomes
451 is maintained, and raises the question of what then maintains sex chromosomes over very
452 long periods of time. In mammals, the high conservation of synteny of the X is thought to be
453 driven by the unusual regulatory architecture of this chromosome due to dosage compensation
454 (Ohno 1967; Brashear et al. 2021). A similar argument may apply to insects, since Muller

455 element F is known not only for its specific regulatory mechanisms, but also for being highly
456 heterochromatic and non-recombining.

457

458 **The conserved heterochromatic nature of the X**

459 Although characterizing the chromatin and recombinational landscape of the *P. cognata* X
460 would require additional data, we estimated several parameters that are often associated with
461 heterochromatic and/or low recombination regions of the genome: genetic diversity, GC
462 content and repeat content. Similarly to the Diptera Muller element F, the *P. cognata* X
463 appears to be to some extent heterochromatic. In particular, we detected dramatically reduced
464 levels of nucleotide diversity on the X relative to the autosomes (X/A ratio well below 0.75 in
465 both sexes), elevated repeat content on the X relative to the autosomes, and reduced GC
466 content of the X compared to the autosomes. The cockroach X, which is also homologous to
467 element F, is heterochromatic over much of its length (Keil and Ross 1984), raising the
468 possibility that this is an ancestral feature that has contributed to the conservation of this sex
469 chromosome over 450 million years. The characterization of the chromatin landscape of
470 various insects that have maintained the ancestral X chromosome will be needed to shed light
471 on whether its unusual epigenetic profile has played a role in its conservation.

472

473 **Partial evidence of demasculinisation of the *P. cognata* X chromosome**

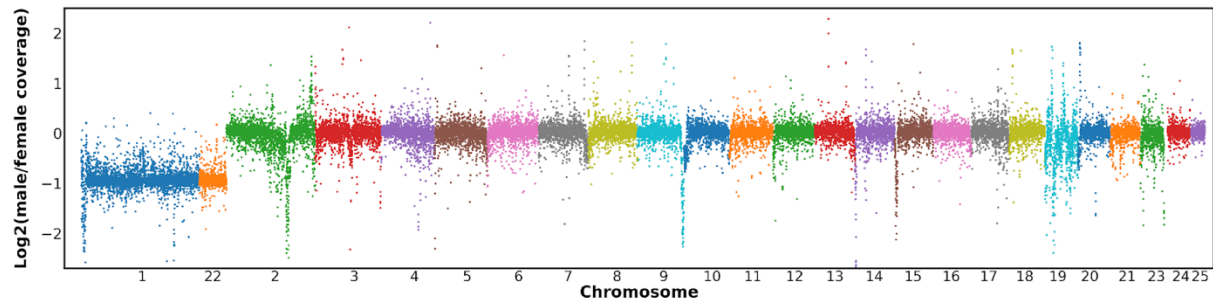
474 As the X chromosome spends twice as much time in females as in males, sexually
475 antagonistic selection may favour the accumulation of female-beneficial mutations on the X
476 chromosome (Rice 1984; Connallon and Clark 2010). Numerous studies have reported a non-
477 random distribution of genes with sex-biased expression across the genome, with a
478 demasculinisation of the X in numerous taxa, except mammals (Lercher 2003; Zhang et al.
479 2010). In insects, female-biased genes are generally over-represented on the X relative to the
480 autosomes in *Drosophila* and beetles (Prince et al. 2010), and reciprocally, male-biased genes
481 seem to escape the X in these two taxa and in mosquitoes (Diptera) (Betrán et al. 2002; Meisel
482 et al. 2009; Vibranovski et al. 2009; Toups and Hahn 2010; Magnusson et al. 2012; Pease

483 and Hahn 2012). Whether the widespread pattern of demasculinisation of the X in insects is a
484 consequence of selection against genes with male-specific functions, or is simply due to
485 reduced expression of the X in testis, is still unclear. The *P. cognata* X shows mixed evidence
486 of demasculinisation of the X. On the one hand, genes with male-biased expression appeared
487 less prevalent on the X than on the autosomes, but, on the other hand, genes exclusively
488 expressed in testis were equally as common on the X and the autosomes (**Figure 3(e) and**
489 **(f)**). Our results therefore show that genes that function primarily in the testes can survive on
490 the X even when the expression of this chromosome is generally female-biased, perhaps
491 arguing against the hypothesis that selection has driven male-biased genes out of the X.

492

493 **Figures**

494



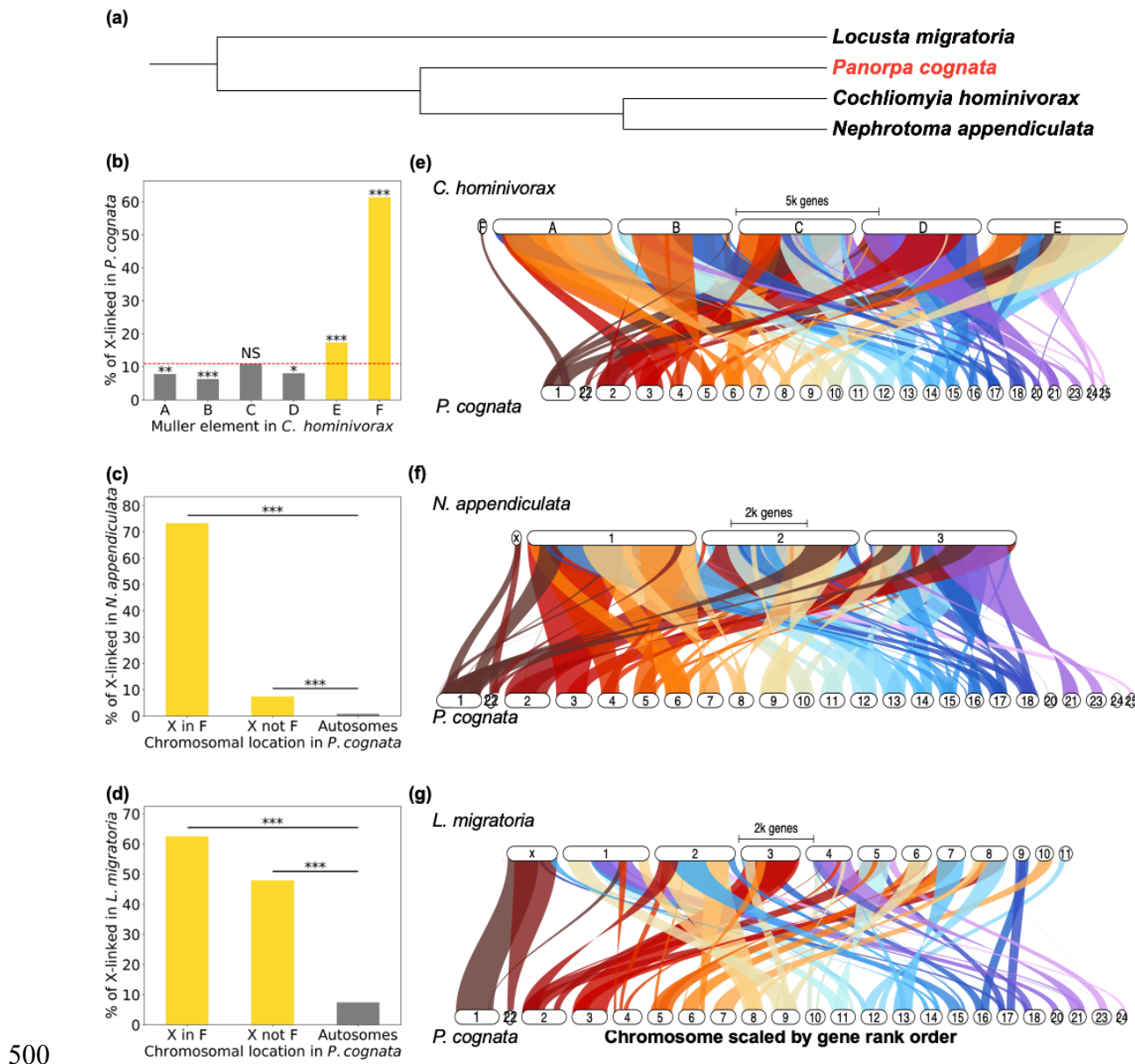
495

496 **Figure 1: Patterns of male/female coverage for the longest 25 scaffolds in 10000 bp**

497 **windows.** Scaffolds 1 and 22 were classified as X-linked based on their reduced

498 male:female coverage ratio.

499

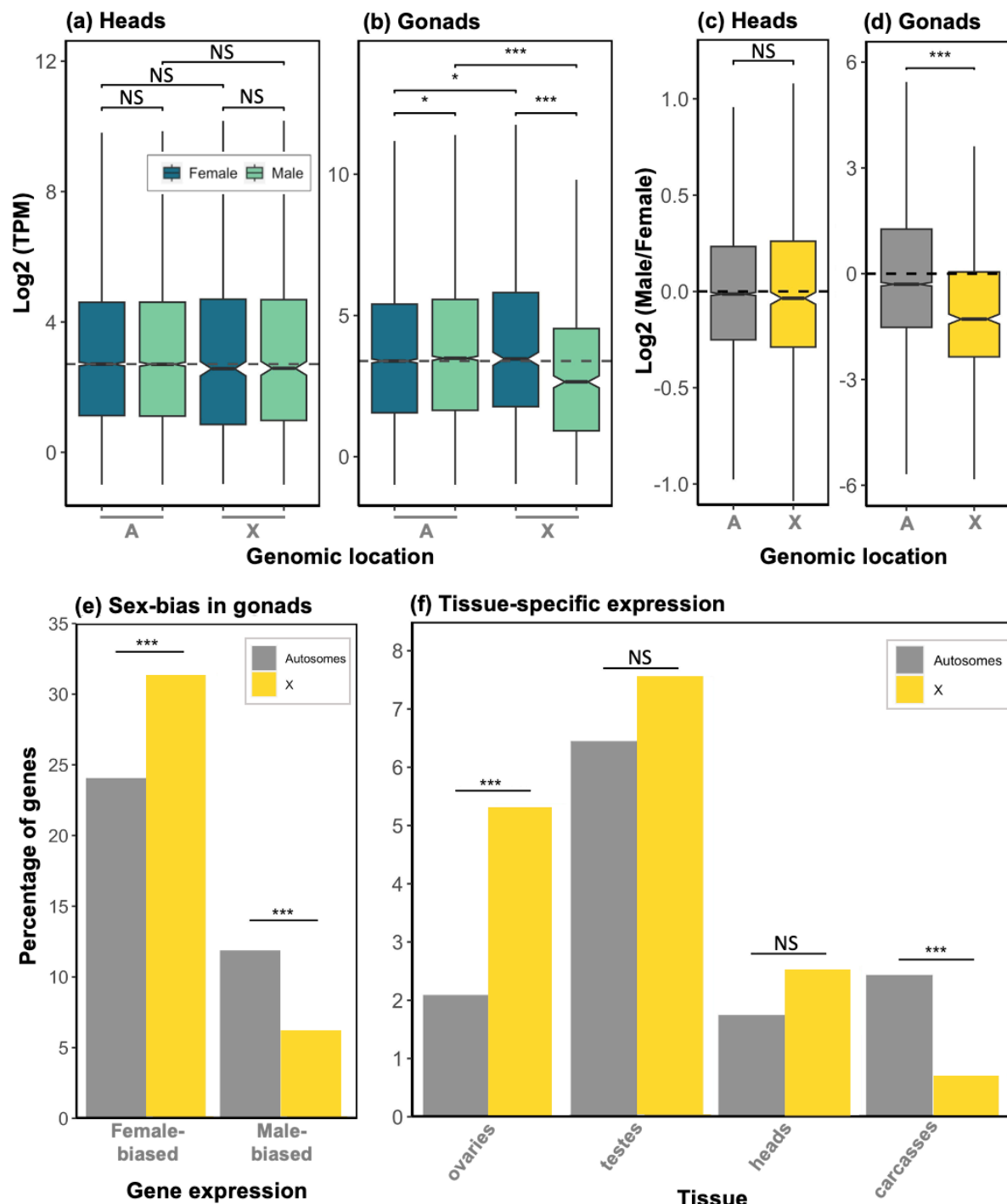


501 **Figure 2: Homology of the X chromosomes of *P. cognata* (order: Mecoptera) and three**
 502 **other insects: two Diptera, *C. hominivorax* (suborder: Brachycera) and *N.***
 503 ***appendiculata* (suborder: Nematocera), and *L. migratoria* (order: Orthoptera).** (a)

504 Phylogenetic tree of the 4 species. (b) Percentage of genes on each of the *C. hominivorax*'s
 505 Muller elements that are X-linked in *P. cognata*. The red dashed line represents the overall
 506 proportion of orthologs that are X-linked in *P. cognata* (i.e. the "X-linkage threshold"). (c)
 507 Percentage of X-linked and autosomal *P. cognata* genes that are X-linked in *N. appendiculata*.
 508 The X-linked genes of *P. cognata* were divided into two sets, based on whether they were F-
 509 linked in *C. hominivorax* (X-in-F), or not (X-not-F). (d) same as (c) but showing the percentage

510 of *P. cognata* genes that are X-linked in *L. migratoria*. Statistically significant differences
 511 between observed and expected percentages were assessed using a chi-squared test (* P
 512 < 0.05 , ** $P < 0.01$, *** $P < 0.001$, NS not significant). (e,f,g) Synteny plots between *P.*
 513 *cognata*'s 25 largest genome scaffolds and the genomes of the 3 other insect species.

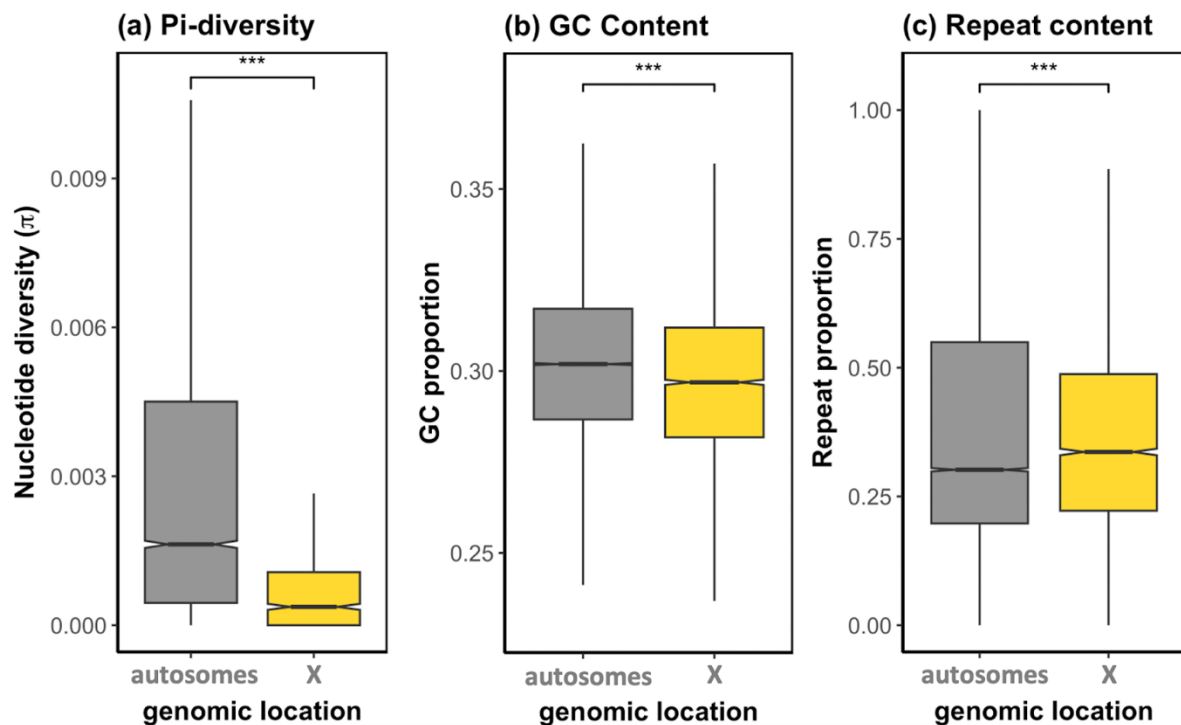
514



515

516 **Figure 3: Dosage compensation and biased gene content of the X.** (a) and (b): expression
517 of autosomal and X-linked genes in males and females, in heads and gonads, respectively
518 (grey dashed line is the female autosomal gene expression median). (c) and (d): \log_2 of male-
519 over-female expression ratios for the autosomal and X-linked genes, in heads and gonads,
520 respectively. Statistically significant differences between groups were assessed using a
521 Wilcoxon rank sum test (* adj. $P < 0.05$, ** adj. $P < 0.01$, *** adj. $P < 0.001$, NS not
522 significant). (e) percentage of autosomal and X-linked genes exhibiting sex-biased expression
523 in gonads. (f) Percentage of autosomal and X-linked genes showing tissue-specific
524 expression. Statistically significant differences between the autosomes and the X in (e) and
525 (f) were assessed using a chi-squared test.

526



528 **Figure 4: X vs. autosomal (a) female nucleotide diversity (π), (b) GC content and (c)**
529 **repeat content (per 10000 bp windows).** Statistically significant differences between groups
530 were assessed using a Wilcoxon rank sum test (* adj. $P < 0.05$, ** adj. $P < 0.01$, *** adj. P
531 < 0.001 , NS not significant).

532

533 **Data accessibility**

534 All raw RNA-seq and DNA-seq data have been uploaded to the NCBI under project
535 PRJNA989034. Processed data files are available at:
536 <https://seafire.ist.ac.at/d/efa3989c33024b859c02/>. Pipelines are available
537 at: <https://github.com/ClemLasne/PanorpaX>

538

539 **Supplementary information:**

540 Please see Supplementary_material_Panorpa_manuscript.pdf

541

542 **Authors' contribution**

543 CL and ME: conceptualization, data curation, formal analysis, methodology, writing—original
544 draft, writing—review and editing; MT and LL: formal analysis, writing—original draft,
545 writing—review and editing; A.M.: methodology, resources; B.V.: conceptualization, formal
546 analysis, funding acquisition, project administration, writing—original draft, writing—review
547 and editing. All authors gave final approval for publication and agreed to be held
548 accountable for the work performed therein.

549

550 **Acknowledgements**

551 We thank the Vicoso lab for their assistance with specimen collection, and Tim Connallon for
552 valuable comments and suggestions on earlier versions of the manuscript. Computational
553 resources and support were provided by the Scientific Computing unit at the ISTA. This
554 research was supported by grants from the Austrian Science Foundation to C.L. (FWF ESP
555 39), and to B.V. (FWF SFB F88-10).

556

557

558 **References**

559 Andrews S. 2010. FastQC: a quality control tool for high throughput sequence data. Available
560 from: <http://www.bioinformatics.babraham.ac.uk/projects/fastqc/>

561 Ashburner M, Golic KG, Hawley RS. 2005. *Drosophila*: a laboratory handbook. 2nd ed. Cold
562 Spring Harbor, N.Y: Cold Spring Harbor Laboratory Press

563 Becking T, Giraud I, Raimond M, Moumen B, Chandler C, Cordaux R, Gilbert C. 2017.
564 Diversity and evolution of sex determination systems in terrestrial isopods. *Sci. Rep.*
565 7:1084.

566 Betrán E, Thornton K, Long M. 2002. Retroposed New Genes Out of the X in *Drosophila*.
567 *Genome Res.* 12:1854–1859.

568 Blackmon H, Ross L, Bachtrog D. 2017. Sex Determination, Sex Chromosomes, and
569 Karyotype Evolution in Insects. *J. Hered.* 108:78–93.

570 Bolger AM, Lohse M, Usadel B. 2014. Trimmomatic: a flexible trimmer for Illumina sequence
571 data. *Bioinformatics* 30:2114–2120.

572 Bracewell R, Tran A, Chatla K, Bachtrog D. 2023. Sex chromosome evolution in beetles.
573 Available from: <http://biorxiv.org/lookup/doi/10.1101/2023.01.18.524646>

574 Brashear WA, Bredemeyer KR, Murphy WJ. 2021. Genomic architecture constrained
575 placental mammal X Chromosome evolution. *Genome Res.* 31:1353–1365.

576 Bray NL, Pimentel H, Melsted P, Pachter L. 2016. Near-optimal probabilistic RNA-seq
577 quantification. *Nat. Biotechnol.* 34:525–527.

578 Camacho C, Coulouris G, Avagyan V, Ma N, Papadopoulos J, Bealer K, Madden TL. 2009.
579 BLAST+: architecture and applications. *BMC Bioinformatics* 10:421.

580 Charlesworth B, Sniegowski P, Stephan W. 1994. The evolutionary dynamics of repetitive
581 DNA in eukaryotes. *Nature* 371:215–220.

582 Charlesworth D, Zhang Y, Bergero R, Graham C, Gardner J, Yong L. 2020. Using GC Content
583 to Compare Recombination Patterns on the Sex Chromosomes and Autosomes of the
584 Guppy, *Poecilia reticulata*, and Its Close Outgroup Species. *Mol. Biol. Evol.* 37:3550–
585 3562.

586 Chauhan P, Swaegers J, Sánchez-Guillén RA, Svensson EI, Wellenreuther M, Hansson B.
587 2021. Genome assembly, sex-biased gene expression and dosage compensation in
588 the damselfly *Ischnura elegans*. *Genomics* 113:1828–1837.

589 Cheng H, Concepcion GT, Feng X, Zhang H, Li H. 2021. Haplotype-resolved de novo
590 assembly using phased assembly graphs with hifiasm. *Nat. Methods* 18:170–175.

591 Connallon T, Clark AG. 2010. SEX LINKAGE, SEX-SPECIFIC SELECTION, AND THE ROLE
592 OF RECOMBINATION IN THE EVOLUTION OF SEXUALLY DIMORPHIC GENE
593 EXPRESSION: SEX LINKAGE AND SEXUAL DIMORPHISM. *Evolution* 64:3417–
594 3442.

595 Danecek P, Auton A, Abecasis G, Albers CA, Banks E, DePristo MA, Handsaker RE, Lunter
596 G, Marth GT, Sherry ST, et al. 2011. The variant call format and VCFtools.
597 *Bioinformatics* 27:2156–2158.

598 Danecek P, Bonfield JK, Liddle J, Marshall J, Ohan V, Pollard MO, Whitwham A, Keane T,
599 McCarthy SA, Davies RM, et al. 2021. Twelve years of SAMtools and BCFtools.
600 *GigaScience* 10:giab008.

601 El Taher A, Ronco F, Matschiner M, Salzburger W, Böhne A. 2021. Dynamics of sex
602 chromosome evolution in a rapid radiation of cichlid fishes. *Sci. Adv.* 7:eabe8215.

603 Emms DM, Kelly S. 2019. OrthoFinder: phylogenetic orthology inference for comparative
604 genomics. *Genome Biol.* 20:238.

605 Fan Z, Ma Q, Ma S, Cao F, Yan R, Lin X. 2023. Maleness-on-the-Y (MoY) orthologue is a key
606 regulator of male sex determination in *Zeugodacus cucurbitae* (Diptera: Tephritidae).
607 *J. Integr. Agric.* 22:505–513.

608 Flynn JM, Hubley R, Goubert C, Rosen J, Clark AG, Feschotte C, Smit AF. 2020.
609 RepeatModeler2 for automated genomic discovery of transposable element families.
610 *Proc. Natl. Acad. Sci.* 117:9451–9457.

611 Gilbert D. 2016. Gene-omes built from mRNA seq not genome DNA. Available from:
612 <http://f1000research.com/posters/5-1695>

613 Gilbert S. 2000. Chromosomal Sex Determination in Drosophila. In: Developmental Biology.
614 6th ed. Sunderland (MA): Sinauer Associates. Available from: <https://www.ncbi-nlm-nih.gov.libraryproxy.ista.ac.at/books/NBK10025/>

616 Grabherr MG, Haas BJ, Yassour M, Levin JZ, Thompson DA, Amit I, Adiconis X, Fan L,
617 Raychowdhury R, Zeng Q, et al. 2011. Full-length transcriptome assembly from RNA-
618 Seq data without a reference genome. *Nat. Biotechnol.* 29:644–652.

619 Guan D, McCarthy SA, Wood J, Howe K, Wang Y, Durbin R. 2020. Identifying and removing
620 haplotypic duplication in primary genome assemblies. *Bioinformatics* 36:2896–2898.

621 Gupta V, Parisi M, Sturgill D, Nuttall R, Doctolero M, Dudko O, Malley J, Eastman PS, Oliver
622 B. 2006. Global analysis of X-chromosome dosage compensation. *J. Biol.* 5:3.

623 Jeffries DL, Lavanchy G, Sermier R, Sredl MJ, Miura I, Borzée A, Barrow LN, Canestrelli D,
624 Crochet P-A, Dufresnes C, et al. 2018. A rapid rate of sex-chromosome turnover and
625 non-random transitions in true frogs. *Nat. Commun.* 9:4088.

626 Keil CB, Ross MH. 1984. C-banded meiotic karyotype of *Blattella germanica* from prophase I
627 cells. *J. Hered.* 75:185–190.

628 Kent WJ. 2002. BLAT —The BLAST -Like Alignment Tool. *Genome Res.* 12:656–664.

629 Kim D, Paggi JM, Park C, Bennett C, Salzberg SL. 2019. Graph-based genome alignment and
630 genotyping with HISAT2 and HISAT-genotype. *Nat. Biotechnol.* 37:907–915.

631 Korunes KL, Samuk K. 2021. PIXY: Unbiased estimation of nucleotide diversity and
632 divergence in the presence of missing data. *Mol. Ecol. Resour.* 21:1359–1368.

633 Kovaka S, Zimin AV, Pertea GM, Razaghi R, Salzberg SL, Pertea M. 2019. Transcriptome
634 assembly from long-read RNA-seq alignments with StringTie2. *Genome Biol.* 20:278.

635 Langmead B, Salzberg SL. 2012. Fast gapped-read alignment with Bowtie 2. *Nat. Methods*
636 9:357–359.

637 Lercher MJ. 2003. Evidence That the Human X Chromosome Is Enriched for Male-Specific
638 but not Female-Specific Genes. *Mol. Biol. Evol.* 20:1113–1116.

639 Li H. 2013. Aligning sequence reads, clone sequences and assembly contigs with BWA-MEM.
640 Available from: <https://arxiv.org/abs/1303.3997>

641 Li X, Mank J, Ban L. 2022. Grasshopper genome reveals long-term conservation of the X
642 chromosome and temporal variation in X chromosome evolution. Available from:
643 <https://www.researchsquare.com/article/rs-2095195/v1>

644 Lovell JT, Sreedasyam A, Schranz ME, Wilson M, Carlson JW, Harkess A, Emms D,
645 Goodstein DM, Schmutz J. 2022. GENESPACE tracks regions of interest and gene
646 copy number variation across multiple genomes. *eLife* 11:e78526.

647 Magnusson K, Lycett GJ, Mendes AM, Lynd A, Papathanos P-A, Crisanti A, Windbichler N.
648 2012. Demasculinization of the *Anopheles gambiae* X chromosome. *BMC Evol. Biol.*
649 12:69.

650 Mangiafico S. 2023. rcompanion: Functions to Support Extension Education Program
651 Evaluation. Available from: <https://CRAN.R-project.org/package=rcompanion/>

652 Manni M, Berkeley MR, Seppey M, Simão FA, Zdobnov EM. 2021. BUSCO Update: Novel
653 and Streamlined Workflows along with Broader and Deeper Phylogenetic Coverage
654 for Scoring of Eukaryotic, Prokaryotic, and Viral Genomes. *Mol. Biol. Evol.* 38:4647–
655 4654.

656 Marshall Graves JA. 2016. Evolution of vertebrate sex chromosomes and dosage
657 compensation. *Nat. Rev. Genet.* 17:33–46.

658 Meccariello A, Salvemini M, Primo P, Hall B, Koskinioti P, Dalíková M, Gravina A, Guciardino
659 MA, Forlenza F, Gregoriou M-E, et al. 2019. *Maleness-on-the-Y (MoY)* orchestrates
660 male sex determination in major agricultural fruit fly pests. *Science* 365:1457–1460.

661 Meisel RP, Delclos PJ, Wexler JR. 2019. The X chromosome of the German cockroach,
662 *Blattella germanica*, is homologous to a fly X chromosome despite 400 million years
663 divergence. *BMC Biol.* 17:100.

664 Meisel RP, Han MV, Hahn MW. 2009. A Complex Suite of Forces Drives Gene Traffic from
665 Drosophila X Chromosomes. *Genome Biol. Evol.* 1:176–188.

666 Miao Y, Wang J, Hua B. 2019. Molecular phylogeny of the scorpionflies Panorpidae (Insecta:
667 Mecoptera) and chromosomal evolution. *Cladistics* 35:385–400.

668 Mikhaylova LM, Nurminsky DI. 2011. Lack of global meiotic sex chromosome inactivation, and
669 paucity of tissue-specific gene expression on the Drosophila X chromosome. *BMC
670 Biol.* 9:29.

671 Misof B, Erpenbeck D, Sauer KP. 2000. Mitochondrial Gene Fragments Suggest Paraphyly of
672 the Genus Panorpa (Mecoptera, Panorpidae). *Mol. Phylogenetic Evol.* 17:76–84.

673 Misof B, Liu S, Meusemann K, Peters RS, Donath A, Mayer C, Frandsen PB, Ware J, Flouri
674 T, Beutel RG, et al. 2014. Phylogenomics resolves the timing and pattern of insect
675 evolution. *Science* 346:763–767.

676 Muller HJ. 1914. A factor for the fourth chromosome of *Drosophila*. *Science* 39:906–906.

677 Ohno S. 1967. Sex Chromosomes and Sex-Linked Genes. Springer. New York, US

678 Pal A, Vicoso B. 2015. The X Chromosome of Hemipteran Insects: Conservation, Dosage
679 Compensation and Sex-Biased Expression. *Genome Biol. Evol.* 7:3259–3268.

680 Parisi M, Nuttall R, Naiman D, Bouffard G, Malley J, Andrews J, Eastman S, Oliver B. 2003.
681 Paucity of Genes on the *Drosophila* X Chromosome Showing Male-Biased Expression.
682 *Science* 299:697–700.

683 Parker DJ, Jaron KS, Dumas Z, Robinson-Rechavi M, Schwander T. 2022. X chromosomes
684 show relaxed selection and complete somatic dosage compensation across *Timema*
685 stick insect species. *J. Evol. Biol.* 35:1734–1750.

686 Pease JB, Hahn MW. 2012. Sex Chromosomes Evolved from Independent Ancestral Linkage
687 Groups in Winged Insects. *Mol. Biol. Evol.* 29:1645–1653.

688 Pertea G, Pertea M. 2020. GFF Utilities: GffRead and GffCompare. *F1000Research* 9:304.

689 Pimentel H, Bray NL, Puente S, Melsted P, Pachter L. 2017. Differential analysis of RNA-seq
690 incorporating quantification uncertainty. *Nat. Methods* 14:687–690.

691 Pokorná M, Kratochvíl L. 2009. Phylogeny of sex-determining mechanisms in squamate
692 reptiles: are sex chromosomes an evolutionary trap? *Zool. J. Linn. Soc.* 156:168–183.

693 Prince EG, Kirkland D, Demuth JP. 2010. Hyperexpression of the X Chromosome in Both
694 Sexes Results in Extensive Female Bias of X-Linked Genes in the Flour Beetle.
695 *Genome Biol. Evol.* 2:336–346.

696 R Core Team. 2020. R: A language and environment for statistical computing. Available from:
697 <https://www.R-project.org/>.

698 Rice WR. 1984. SEX CHROMOSOMES AND THE EVOLUTION OF SEXUAL DIMORPHISM.
699 *Evolution* 38:735–742.

700 Scott M. 2022. A chromosomal-scale reference genome of the New World Screwworm,
701 *Cochliomyia hominivorax*. :618269886 bytes. Available from:
702 <https://datadryad.org/stash/dataset/doi:10.5061/dryad.d7wm37q4j>

703 Servant N, Varoquaux N, Lajoie BR, Viara E, Chen C-J, Vert J-P, Heard E, Dekker J, Barillot
704 E. 2015. HiC-Pro: an optimized and flexible pipeline for Hi-C data processing. *Genome*
705 *Biol.* 16:259.

706 Sharma A, Heinze SD, Wu Y, Kohlbrenner T, Morilla I, Brunner C, Wimmer EA, Van De Zande
707 L, Robinson MD, Beukeboom LW, et al. 2017. Male sex in houseflies is determined by
708 *Mdmd*, a paralog of the generic splice factor gene *CWC22*. *Science* 356:642–645.

709 Smit A, Hubley R, Green P. 2013. RepeatMasker Open-4.0. Available from:
710 <http://www.repeatmasker.org>

711 Tandonnet S, Krsticevic F, Basika T, Papathanos PA, Torres TT, Scott MJ. 2023. A
712 chromosomal-scale reference genome of the New World Screwworm, *Cochliomyia*
713 *hominivorax*. *DNA Res.* 30:dsac042.

714 The UniProt Consortium, Bateman A, Martin M-J, Orchard S, Magrane M, Ahmad S, Alpi E,
715 Bowler-Barnett EH, Britto R, Bye-A-Jee H, et al. 2023. UniProt: the Universal Protein
716 Knowledgebase in 2023. *Nucleic Acids Res.* 51:D523–D531.

717 Toups MA, Hahn MW. 2010. Retrogenes Reveal the Direction of Sex-Chromosome Evolution
718 in Mosquitoes. *Genetics* 186:763–766.

719 Toups MA, Vicoso B. 2023. The X chromosome of insects predates the origin of Class Insecta.
720 Available from: <http://biorxiv.org/lookup/doi/10.1101/2023.04.19.537501>

721 Trapnell C, Williams BA, Pertea G, Mortazavi A, Kwan G, Van Baren MJ, Salzberg SL, Wold
722 BJ, Pachter L. 2010. Transcript assembly and quantification by RNA-Seq reveals
723 unannotated transcripts and isoform switching during cell differentiation. *Nat.*
724 *Biotechnol.* 28:511–515.

725 Vibranovski MD, Zhang Y, Long M. 2009. General gene movement off the X chromosome in
726 the *Drosophila* genus. *Genome Res.* 19:897–903.

727 Vicoso B. 2019. Molecular and evolutionary dynamics of animal sex-chromosome turnover.
728 *Nat. Ecol. Evol.* 3:1632–1641.

729 Vicoso B, Bachtrog D. 2013. Reversal of an ancient sex chromosome to an autosome in
730 *Drosophila*. *Nature* 499:332–335.

731 Vicoso B, Bachtrog D. 2015. Numerous Transitions of Sex Chromosomes in Diptera. *PLOS*
732 *Biol.* 13:e1002078.

733 Virtanen P, Gommers R, Oliphant TE, Haberland M, Reddy T, Cournapeau D, Burovski E,
734 Peterson P, Weckesser W, Bright J, et al. 2020. SciPy 1.0: fundamental algorithms for
735 scientific computing in Python. *Nat. Methods* 17:261–272.

736 Whittle CA, Kulkarni A, Extavour CG. 2020. Absence of a Faster-X Effect in Beetles (*Tribolium*
737 , Coleoptera). *G3 GenesGenomesGenetics* 10:1125–1136.

738 Willforss J, Chawade A, Levander F. 2019. NormalizerDE: Online Tool for Improved
739 Normalization of Omics Expression Data and High-Sensitivity Differential Expression
740 Analysis. *J. Proteome Res.* 18:732–740.

741 Xu B, Li Y, Hua B. 2013. A chromosomal investigation of four species of Chinese Panorpidae
742 (Insecta, Mecoptera). *Comp. Cytogenet.* 7:229–239.

743 Zhang YE, Vibranovski MD, Landback P, Marais GAB, Long M. 2010. Chromosomal
744 Redistribution of Male-Biased Genes in Mammalian Evolution with Two Bursts of Gene
745 Gain on the X Chromosome. *PLoS Biol.* 8:e1000494.

746 Zhou C, McCarthy SA, Durbin R. 2023. YaHS: yet another Hi-C scaffolding tool. *Bioinformatics*
747 39:btac808.

748